



INVESTIGATING THE STEADY STATE STABILITY OF THE NIGERIAN 48- BUS SYSTEMS USING FACTS DEVICES

I. E. Nkan^{1,*}, O. I. Okoro², C. C. Awah³ and U. B. Akuru⁴

¹, DEPT. OF ELECTRICAL/ELECTRONIC ENGR'G, AKWA IBOM STATE UNIV., MPAT-ENIN, AKWA IBOM STATE, NIGERIA

^{2,3} DEPT. OF ELECTRICAL/ELECTRONIC ENGR'G, MICHAEL OKPARA UNIV. OF AGRICULTURE, UMUDIKE, NIGERIA

⁴, EMLAB (ELECTRICAL MACHINES LAB) | E260 DEPARTEMENT OF ELECTRICAL AND ELECTRONIC ENGINEERING, STELLENBOSCH UNIVERSITY, STELLENBOSCH, 7600, SOUTH AFRICA

E-mail addresses: ¹ imoenkan@yahoo.com, ² oiokoro@yahoo.co.uk, ³ ccawah@ieee.org,
⁴ 18375243@sun.ac.za

ABSTRACT

With the ongoing expansions and growth of the electric utility industry, including deregulation in Nigeria, numerous changes characterized by additional generating stations, increase in transmission lines and loads are experienced thereby pushing the transmission systems closer to their stability and thermal limits and hence, causing the transfer of reactive power during steady state operating conditions to constitute a major problem of voltage instability. Flexible ac transmission systems (FACTS) controllers have been utilized for finding solutions to various power system stability control issues such as voltage instability. This paper uses Static Synchronous Series Compensator (SSSC) and Thyristor Controlled Series Compensator (TCSC) to investigate the voltage magnitude profile, active and reactive power losses of the Nigerian 48-bus power system network for steady state stability enhancement using power system analysis toolbox (PSAT) in MATLAB environment. Optimal location of the FACTS devices was achieved through the computation of the voltage stability sensitivity factors (VSSF) for all the buses after continuation power flow (CPF) was carried out. Simulation results obtained without and with the FACTS devices revealed that the two FACTS devices especially TCSC has the capability to raise voltage profile of the buses and mitigate against power losses.

Keywords: CPF, FACTS, MATLAB, Optimal location, PSAT, SSSC, stability, TCSC, VSSF

1. INTRODUCTION

Power system stability is the ability of an electric power system, for a given initial operating condition, to regain a state of operating equilibrium after being subjected to a physical disturbance [1]. In voltage stability, this entails the ability of a power system to maintain an acceptable voltage profile throughout all the buses in the power system under normal condition and after experiencing a perturbation in the power network. A system enters a condition of voltage instability when a disturbance causes an increase in load demand or change in the system condition causes progressive and uncontrollable decline in voltage [2]. Now, more than ever, advanced technologies paramount for the reliable and secure operations of

power systems [3] based on power electronics equipment called FACTS (Flexible AC Transmission Systems), provide proven technical solutions to address the operating challenges of power system instability being presented today. FACTS technologies allow for improved transmission system operation compared to the construction of new transmission lines. In [4], voltage collapse proximity index was computed for optimal placement of Thyristor Controlled Series Compensator (TCSC) and Static Synchronous Compensator (STATCOM) modeled in the IEEE 14 bus system using Power System Analysis Toolbox (PSAT) in MATLAB for improvement in the voltage stability of the system. In [5] also, reactive power loss sensitivity factor method was employed to

find out the best possible location of TCSC and Static Var Compensator (SVC) using power world simulator 8.0 on modified IEEE 9 bus system. Application of SVC using Owerri Transmission Company as case study for enhancement of power system voltage stability with the aid of reactive/capacitive power switching mechanism was presented in [6]. In [7], 28 bus, 330 kV Nigerian transmission system was modeled for the comparison of the voltage enhancement and loss reduction capabilities of STATCOM and Static Synchronous Series Compensator (SSSC) FACTS Controllers using MATLAB based programs. An overview of placement of TCSC for enhancement of power system stability was presented in [8]. Here, differential evolution technique was employed for the minimization of transmission losses and enhancement of stability of the power system. In [9], a systematic modular approach to incorporate series and shunt FACTS controllers in differential algebraic equation (DAE) model of multimachine power system in coordinated control manner for voltage stability analysis using MATLAB toolbox was presented. [10] reviewed the series and shunt compensation techniques in their discussion of the Nigerian 330 kV transmission system associated with various small signal perturbations in Nigeria power system. In [11], STATCOM was optimally placed in the Nigerian 330 kV, 30-bus system using ant colony optimization meta-heuristic technique for stability in the voltage profile of the buses. In [12], Unified Power Flow Controller (UPFC) was applied to Nigeria's 330 kV, 28-bus transmission system using MATLAB to minimize prolonged and frequent voltage instability in the network and enhance stability while in [13], Newton Raphson power flow iteration method using MATLAB was adopted to optimally placed SSSC in the Nigerian 28-bus system to control voltage magnitude at low voltage buses. In this paper, PSAT software will be used to model a larger Nigerian power system of 48 buses [18], 16 PV generators for load flow studies with 79 transmission lines which reflect the true nature of the ever expanding power system in Nigeria. Simulation studies will be carried out with the application of TCSC and SSSC to investigate the steady state stability of the system for improved system performance.

2. MODELING OF TCSC AND SSSC

2.1 TCSC

The functional model of TCSC is represented in Figure 1 with the terminals of the controller at T_k and T_m. The

fundamental frequency operation can be represented by the following set of equations, which includes the control system equations and sinusoidal currents in the controller.

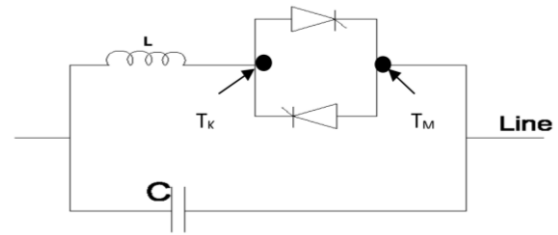


Figure 1: Thyristor Controlled Series Capacitor [14]

$$[x'_c, \alpha']^T = f(x_c, \alpha, I, I_{ref}) \tag{1}$$

$$P + V_k V_m B_e \sin(\delta_k - \delta_m) = 0 \tag{2}$$

$$-V_k^2 B_e + V_k V_m B_e \cos(\delta_k - \delta_m) - Q_k = 0 \tag{3}$$

$$-V_m^2 B_e + V_k V_m B_e \cos(\delta_k - \delta_m) - Q_m = 0 \tag{4}$$

$$B_e - B_e(\alpha) = 0 \tag{5}$$

$$(P^2 + Q_k^2)^{\frac{1}{2}} - IV_k = 0 \tag{6}$$

where x_c and $f(x_c, \alpha, I, I_{ref})$ stand for the internal control system variables and equations. x_c is the constant reactance TCSC model, α is the firing angle TCSC model, B is the series susceptance of the TCSC, V_k and V_m are the terminal voltages of controller, δ_k and δ_m are the magnitudes of the angles at the controller terminals, Q_k and Q_m are the reactive power injections at both controller terminals, P and I are the active power and current flowing through the controller respectively, B_e is given as [14].

$$B_e(\alpha) = \pi(k_x^4 - 2k_x^2 + 1) \cos k_x(\pi - \alpha) + [X_c(\pi k_x^4 \cos k_x(\pi - \alpha) - \pi \cos(k_x - \alpha) - 2k_x^4 \alpha \cos k_x(\pi - \alpha))] \tag{7}$$

Where

$$k_x (\text{Percentage of compensation of TCSC}) = \left(\frac{X_c}{X_L}\right)^{\frac{1}{2}}$$

For an impedance control model with no droop, which yields the simplest set of steady state equations from the numerical point of view, the power flow equations for the TCSC are

$$B_e - B_{ref} = 0 \tag{8}$$

$$P + V_k V_m B_e \sin(\delta_k - \delta_m) = 0 \tag{9}$$

$$-V_k^2 B_e + V_k V_m B_e \cos(\delta_k - \delta_m) - Q_k = 0 \tag{10}$$

$$B_e - B_e(\alpha) = 0 \tag{11}$$

$$(P^2 + Q_k^2)^{\frac{1}{2}} - IV_k = 0 \tag{12}$$

2.2 SSSC

The functional model of SSSC is shown in Figure 2. The SSSC is a series voltage source equipped with a source of energy in the DC link that can supply or absorb the reactive and active power to or from the line [16].

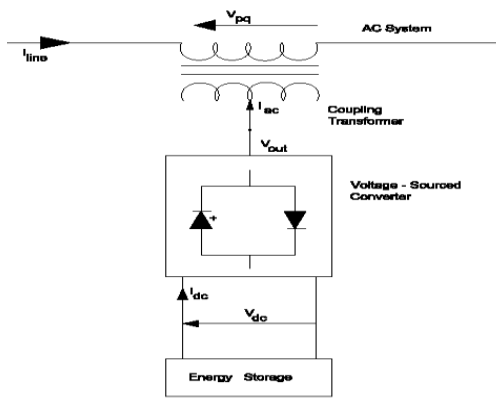


Figure 2: Functional Model of Static Synchronous Series Compensator [15]

2.2.1. Active power flow control

The active power flow constraint is as follows [17]

$$P_{ji} - P_{ji}^{ref} = 0 \tag{13}$$

where P_{ji}^{ref} is the specified active power flow control reference along the line between bus j and i, and P_{ji} is the active power flow given as;

$$P_{ij} = V_i^2 g_{ii} - V_i V_j (g_{ij} \cos \theta_{ij} + b_{ij} \sin \theta_{ij}) - V_i V_{se} (g_{ij} \cos(\theta_i - \theta_{se}) + b_{ij} \sin(\theta_i - \theta_{se})) \tag{14}$$

Where $g_{ij} + j b_{ij} = \frac{1}{Z_{se}}$, $g_{ii} = g_{ij}$, $b_{ii} = b_{ij}$, $g_{jj} = g_{ij}$, $b_{jj} = . b_{ij}$; V_{se} and Z_{se} are the voltage source and impedance sources respectively.

2.2.2. Reactive power flow control

The reactive power flow constraint is as follows;

$$Q_{ji} - Q_{ji}^{ref} = 0 \tag{15}$$

where Q_{ji}^{ref} is the specified reactive power flow control reference, Q_{ji} is the SSSC branch reactive power flows and

$$Q_{ij} = V_i^2 b_{ij} - V_i V_j (g_{ij} \sin \theta_{ij} - b_{ij} \cos \theta_{ij}) - V_i V_{se} (g_{ij} \sin(\theta_i - \theta_{se}) - b_{ij} \cos(\theta_i - \theta_{se})) \tag{16}$$

2.2.3. Bus Voltage Control

The bus voltage control constraints is given as;

$$V_i - V_i^{ref} = 0, V_j^{ref} - V_j = 0 \tag{17}$$

where V_i^{ref} and V_j^{ref} are the bus voltage references.

2.2.4. Reactance Control

In this control function, V_{se} is regulated to control equivalent reactance of the SSSC to a specified reactance reference;

$$I_{se} = I_{ji} = \sqrt{\frac{V_i^2 + V_{se}^2 + V_j^2 - 2V_i V_{se} \cos(\theta_i - \theta_{se}) + 2V_i V_{se} \cos(\theta_i - \theta_{se}) - 2V_i V_j \cos(\theta_i - \theta_{se})}{|Z_{se}|}} \tag{22}$$

$$X_c - X_c^{ref} = 0 \tag{18}$$

where X_c^{ref} is the reference reactance, X_c is the function of state variables V_i, V_j and V_{se} . The objective function can be written as

$$\Delta F(x) = F(x) - F^{ref} = 0 \tag{19}$$

where $x = [\theta_i, \theta_j, \theta_{se}, V_i, V_j, V_{se}]^t$

2.2.5. Voltage and Current Constraints of the SSSC

The equivalent voltage injection V_{se} bound constraint is

$$0 \leq V_{se} \leq V_{se}^{max} \tag{20}$$

where V_{se}^{max} is the voltage rating of V_{se} , which may be constant or change slightly with the changes in the DC bus voltage, depending on the inverter design.

The current through each series converter should be within its current rating:

$$I_{se} \leq I_{se}^{max} \tag{21}$$

where I_{se}^{max} is the current rating of the series converter. But $I_{se} = I_{se} < \theta_{se} = \frac{V_i - V_{se} - V_j}{Z_{se}}$, the actual current magnitude through the SSSC can be obtained as (22).

3. MODELING OF THE NIGERIAN 48-BUS SYSTEM

Using PSAT software in MATLAB, modeling of the systems shown in Figures 3 and 4 were achieved with the optimal placement of TCSC and SSSC on line 3-4 in the 48-bus system of Nigeria which comprises of 16 PV generators for load flow studies, 79 transmission lines and 32 load buses obtained from the Transmission Company of Nigeria, National Control Centre, Oshogbo.

Kano transmission station at bus 4 had experienced very low voltage during load flow calculations, hence the need to place the FACTS devices on line 3-4. Tables 1 and 2 show all the data for the 48 buses and transmission lines respectively.

4. SIMULATION RESULTS OF NIGERIAN 48-BUS SYSTEM

The steady state performances of TCSC and SSSC are here presented by the outcome of the voltage magnitude profile at the buses, the real and reactive power losses experienced at the transmission lines.

Newton Raphson power flow simulations were carried out on the modeled Nigerian 48-Bus systems of Figures 3 and 4 first without FACTS and thereafter with TCSC and SSSC. In 0.156 second, the systems without FACTS and with SSSC converges at 2.9437 e-09 p.u. and 1.6667 e-10 p.u. respectively after 4 iterations while the system with TCSC converges at 9.6232 e-11 p.u. after 4 iterations in 0.687 second. The summaries of the results of the power flow are shown in Tables 3 and 6. Table 4 shows the results of the continuation power flow (CPF) where the load at the buses were increased successively until the critical loading parameter was reached. Following the successful completion of power flow and CPF simulations for the

Nigerian 48-bus system, voltage stability sensitivity factors (VSSF) were computed for all the load buses as displayed in Table 5. The result of the CPF is completed in 2.0922 seconds with maximum loading parameter (λ_{max}) equaling 3.1887. Taking a look at Table 4, it can be observed that buses 3(Kaduna), 4(Kano), 6(Makurdi), 9(Jos), 13(Osogbo), 22(Ugwuaji) and 28(Ayede) were found to be very weak buses with voltages well below 0.800 p.u. Bus 4(Kano) is noticed to be the weakest bus with voltage magnitude of 0.36128 p.u. From Table 5 (VSSF), Bus 4(Kano) is also seen to have the highest factor of 0.57724 and therefore, the weakest bus and most suitable for the installation of TCSC and SSSC.

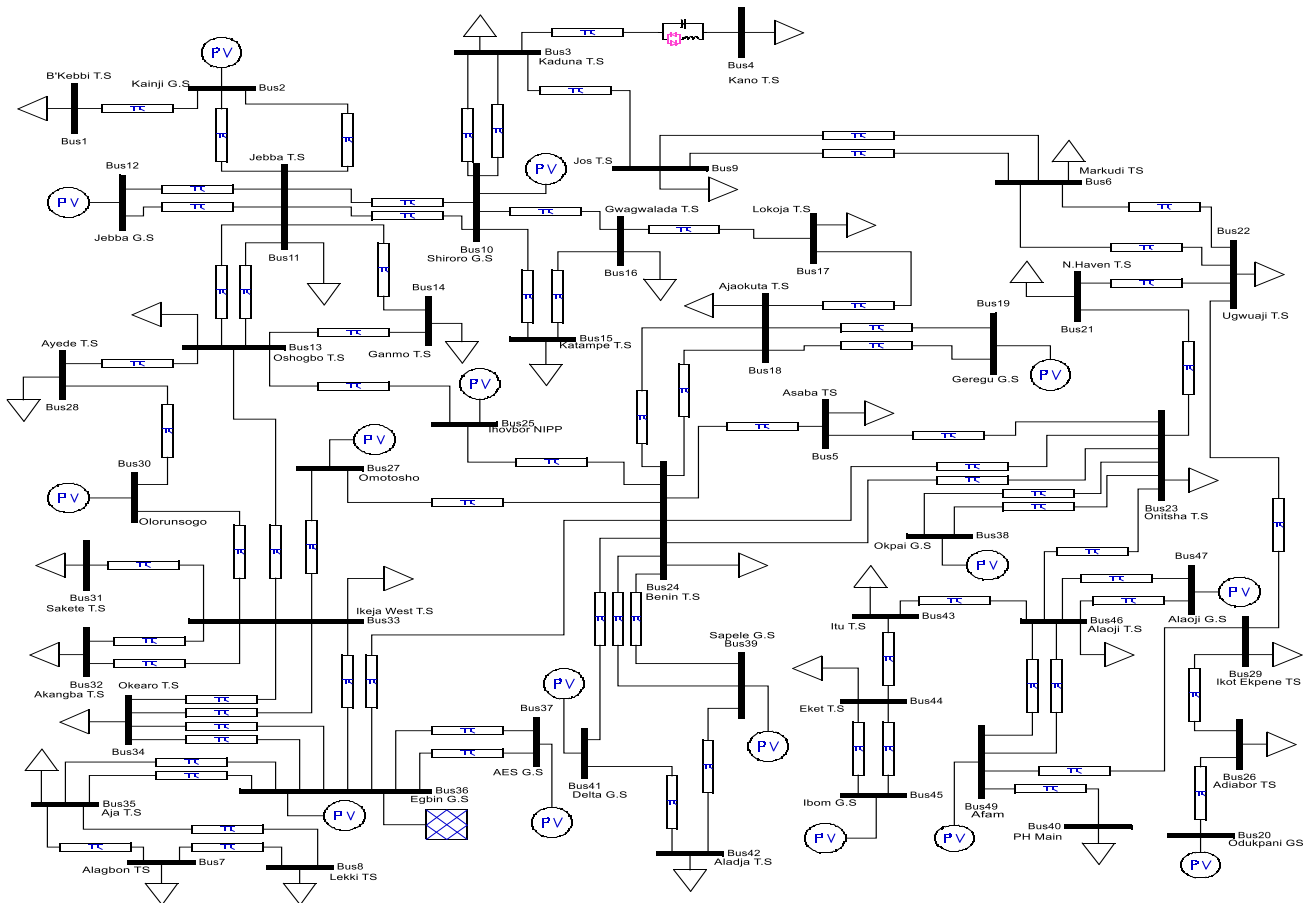


Figure 3: Nigerian 48-bus system with TCSC placed on line 3-4

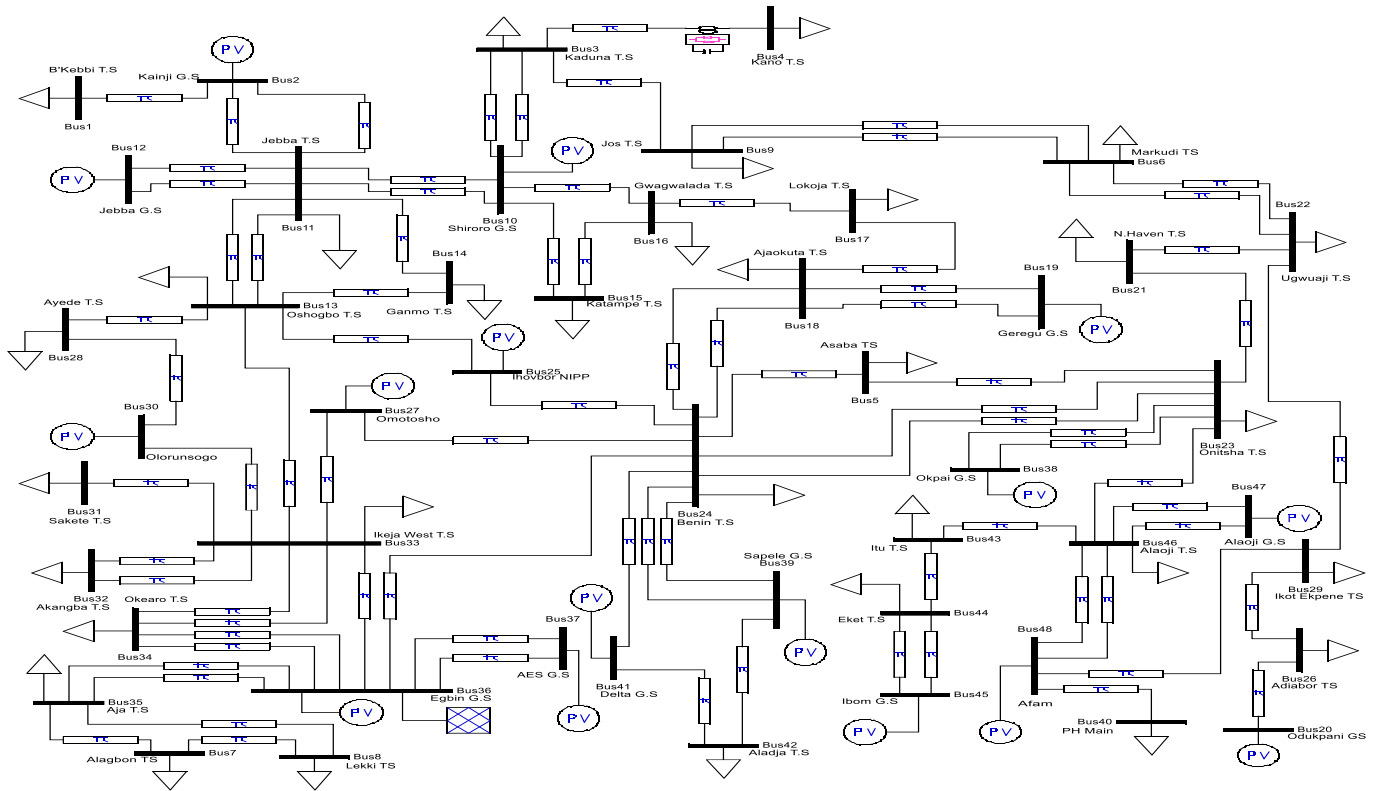


Figure 4: Nigerian 48-bus system with SSSC placed on line 3-4

Table 1: Bus data for Nigerian 48-bus system

BUS NO	BUS NAME	NOM VOLT (kV)	ACTUAL VOLT (kV)	VOLT MAG. (PU)	LOAD		GENERATION	
					MW	MVAR	MW	MVAR
1	Birnin Kebbi	330	326	0.988	100	62	-	-
2	Kainji GS	330	330	1.0	-	-	492	158
3	Kaduna	330	315	0.956	120	90	-	-
4	Kano	330	300	0.909	41	26	-	-
5	Asaba	330	305	0.924	80	59	-	-
6	Markudi	330	310	0.939	100	60	-	-
7	Alagbon	330	320	0.97	70	43	-	-
8	Lekki	330	300	0.909	110	78	-	-
9	Jos	330	310	0.939	160	70	-	-
10	Shiroro GS	330	330	1.0	-	-	500	115
11	Jebba	330	326	0.988	260	195	-	-
12	Jebba GS	330	330	1.0	-	-	403	190
13	Oshogbo	330	330	1.0	127	95	-	-
14	Ganmo	330	328	0.994	100	75	-	-
15	Katampe	330	330	1.0	303	227	-	-
16	Gwagwalada	330	315	0.956	220	165	-	-
17	Lokoja	330	320	0.97	120	90	-	-
18	Ajaokuta	330	320	0.97	120	90	-	-
19	Geregu GS	330	330	1.0	-	-	531	230
20	Odukpani GS	330	330	1.0	-	-	260	121
21	New Heaven	330	326	0.988	196	147	-	-
22	Ugwuaji	330	328	0.994	175	131	-	-

BUS NO	BUS NAME	NOM VOLT (kV)	ACTUAL VOLT (kV)	VOLT MAG. (PU)	LOAD		GENERATION	
					MW	MVAR	MW	MVAR
23	Onitsha	330	324	0.982	100	75	-	-
24	Benin	330	328	0.994	144	108	-	-
25	Ihovbor GS	330	330	1.0	-	-	117	71
26	Adiabor	330	320	0.97	90	48	-	-
27	Omotosho GS	330	330	1.0	-	-	165	73
28	Ayede	330	320	0.97	190	151	-	-
29	Ikot Ekpene	330	313	0.948	165	74	-	-
30	Olorunsogo GS	330	330	1.0	-	-	196	124
31	Sakete	330	300	0.909	225	190	-	-
32	Akangba	330	330	1.0	203	152	-	-
33	Ikeja West	330	330	1.0	847	635	-	-
34	Okearo	330	330	1.0	120	90	-	-
35	Aja	330	330	1.0	120	90	-	-
36	Egbin GS	330	330	1.0	-	-	513	240
37	AES GS	330	330	1.0	-	-	245	195
38	Okpai GS	330	330	1.0	-	-	466	200
39	Sapele GS	330	330	1.0	-	-	178	79
40	PH Main	330	300	0.909	280	140	-	-
41	Delta GS	330	330	1.0	-	-	341	115
42	Aladja	330	325	0.985	210	158	-	-
43	Itu	330	330	1.0	199	91	-	-
44	Eket	330	328	0.994	200	147	-	-
45	Ibom GS	330	330	1.0	-	-	31	12
46	Alaoji	330	320	0.97	240	100	-	-
47	Alaoji GS	330	330	1.0	-	-	250	117
48	Afam GS	330	321	0.973	-	-	700	506

Source [18]

Table 2: Line data for Nigerian 48-bus system on 100MVA, 330kV, 50Hz

S/N	FROM BUS	TO BUS	R (PU)	X (PU)	1/2 B (PU)	S/N	FROM BUS	TO BUS	R (PU)	X (PU)	1/2 B (PU)
1	1	2	0.0011019	0.0142241	0.064172	21	11	12	0.0002890	0.0022300	0.404978
2	2	11	0.0039008	0.0246198	0.036385	22	11	12	0.0002890	0.0022300	0.404978
3	2	11	0.0039008	0.0246198	0.036385	23	11	13	0.0056226	0.0477199	0.018980
4	3	4	0.0030370	0.0300082	0.030295	24	11	13	0.0056226	0.0477199	0.018980
5	3	9	0.0022193	0.0115139	0.076896	25	11	14	0.0039390	0.0133430	0.063304
6	3	10	0.0094380	0.0391791	0.022152	26	13	14	0.0016834	0.0142860	0.063398
7	3	10	0.0094380	0.0391791	0.022152	27	13	25	0.0089890	0.0762910	0.011872
8	5	23	0.0017171	0.0145744	0.062143	28	13	28	0.0041185	0.0349541	0.025911
9	5	24	0.0031889	0.0270666	0.003248	29	13	33	0.0089532	0.0759871	0.011919
10	6	9	0.0053470	0.0195760	0.043652	30	15	16	0.0016050	0.0300600	0.002826
11	6	9	0.0053470	0.0195760	0.043652	31	16	17	0.0043170	0.0015800	0.068655
12	6	22	0.0064850	0.0553970	0.016352	32	17	18	0.0017150	0.0131860	0.068482
13	6	22	0.0064850	0.0553970	0.016352	33	18	19	0.0000540	0.0005100	1.780575
14	7	8	0.0091700	0.0292470	0.028587	34	18	19	0.0000540	0.0005100	1.780575
15	7	35	0.0009410	0.0072340	0.124826	35	18	24	0.0070551	0.0542562	0.016643
16	8	35	0.0049670	0.0157480	0.053035	36	18	24	0.0070551	0.0542562	0.016643
17	10	11	0.0087383	0.0741635	0.012212	37	20	26	0.0005770	0.0048910	0.185171
18	10	11	0.0087383	0.0741635	0.012212	38	21	22	0.0002530	0.0019480	0.463574
19	10	15	0.0048872	0.0106557	0.071355	39	21	23	0.0002380	0.0004321	1.604128
20	10	16	0.0052820	0.0106200	0.069319	40	22	29	0.0059210	0.0219100	0.039059
						41	23	24	0.0049063	0.0416410	0.021750

S/N	FROM BUS	TO BUS	R (PU)	X (PU)	1/2 B (PU)
42	23	24	0.0049063	0.0416410	0.021750
43	23	38	0.0021708	0.0166942	0.082468
44	23	38	0.0021708	0.0166942	0.082468
45	23	46	0.0049422	0.0419449	0.021593
46	24	25	0.0008990	0.0076200	0.118854
47	24	27	0.0018264	0.0155014	0.059169
48	24	36	0.0071025	0.0607897	0.014902
49	24	39	0.0018090	0.0139118	0.064909
50	24	39	0.0018090	0.0139118	0.064909
51	24	41	0.0014683	0.0124619	0.072678
52	26	29	0.0021880	0.0185740	0.048762
53	27	33	0.0028640	0.0243150	0.037249
54	28	30	0.0021488	0.0182369	0.049663
55	29	48	0.0023030	0.0195500	0.046328
56	30	33	0.0027566	0.0234030	0.039234
57	31	33	0.0025069	0.0212764	0.042568
58	32	33	0.0006151	0.0047300	0.190909
59	32	33	0.0006151	0.0047300	0.190909
60	33	34	0.0006450	0.0054710	0.165543
61	33	34	0.0006450	0.0054710	0.165543
62	33	36	0.0006450	0.0054710	0.165543
63	34	36	0.0006450	0.0054710	0.165543
64	34	36	0.0006450	0.0054710	0.165543
65	35	36	0.0005014	0.0042553	0.939551
66	35	36	0.0005014	0.0042553	0.939551
67	36	37	0.0071625	0.0607897	0.014899
68	36	37	0.0071625	0.0607897	0.014899
69	39	42	0.0022562	0.0191488	0.047298
70	40	48	0.0009045	0.0069559	0.129819
71	41	42	0.0011460	0.0097264	0.093118
72	43	44	0.0009045	0.0069559	0.129819
73	43	46	0.0009045	0.0069559	0.129819
74	44	45	0.0009045	0.0069559	0.129819
75	44	45	0.0009045	0.0069559	0.129819
76	46	47	0.0049422	0.0419449	0.021593
77	46	47	0.0049422	0.0419449	0.021593
78	46	48	0.0009045	0.0069559	0.129819
79	46	48	0.0009045	0.0069559	0.129819

Source [18]

Table 3: Power flow results of Nigerian 48-Bus system without FACTS

BUS NO	BUS NAME	VOLTAGE (pu)	PHASE ANGLE (rad)	REAL POWER (pu)	REACTIVE POWER (pu)
1	Birin Kebbi	0.9899	0.1273	-1	-0.62
2	Kainji GS	1.0	0.1410	4.92	0.5016
3	Kaduna	0.9482	-0.0020	-1.2	-0.9
4	Kano	0.9385	-0.0149	-0.41	-0.26
5	Asaba	0.9745	0.0369	-0.8	-0.59
6	Makurdi	0.9405	-0.0107	-1.0	-0.6
7	Alagbon	1.0225	-0.0113	-0.7	-0.43
8	Lekki	1.0146	-0.0160	-1.1	-0.78
9	Jos	0.9381	-0.0154	-1.6	-0.7
10	Shiroro GS	1.0	0.0463	5.0	6.3177
11	Jebba	0.9955	0.0923	-2.6	-1.95
12	Jebba GS	1.0	0.0962	4.03	3.77
13	Oshogbo	0.9716	0.0477	-1.27	-0.95
14	Ganmo	0.9747	0.0655	-1.0	-0.75
15	Katampe	0.969	0.0382	-3.03	-2.27

BUS NO	BUS NAME	VOLTAGE (pu)	PHASE ANGLE (rad)	REAL POWER (pu)	REACTIVE POWER (pu)
16	Gwagwalada	0.9713	0.0383	-2.2	-1.65
17	Lokoja	0.9800	0.0413	-1.2	-0.9
18	Ajaokuta	0.9993	0.0819	-1.2	-0.9
19	Geregu GS	1.0	0.0832	5.31	2.0461
20	Odukpani GS	1.0	0.0842	2.6	0.9802
21	New heaven	0.9709	0.0361	-1.96	-1.47
22	Ugwuaji	0.9670	0.031	-1.75	-1.31
23	Onitsha	0.9734	0.0374	-1.0	-0.75
24	Benin	0.9956	0.0562	-1.44	-1.08
25	Ihovbor GS	1.0	0.0629	1.166	0.8111
26	Adiabor	0.9938	0.0719	-0.9	-0.48
27	Omosho GS	1.006	0.0412	1.65	0.9512
28	Ayede	0.9483	0.0036	-1.9	-1.51
29	Ikot Ekpene	0.9819	0.0407	-1.65	-0.74
30	Olorunsogo GS	0.97	0.0148	1.96	-0.1507
31	Sakete	0.9469	-0.0653	-2.25	-1.9
32	Akangba	0.9923	-0.0240	-2.03	-1.52
33	Ikeja West	0.9966	-0.0196	-8.47	-6.35
34	Okearo	1.0133	-0.0111	-1.2	-0.9
35	Aja	1.0278	-0.0055	-1.2	-0.9
36	Egbin GS	1.033	0.0	9.2005	17.6746
37	AES GS	1.0	0.0766	2.452	-1.2759
38	Okpai GS	1.0	0.0744	4.66	2.6555
39	Sapele GS	1.0	0.0658	1.78	0.9291
40	PH Main	0.9874	0.0306	-2.8	-1.4
41	Delta GS	1.003	0.0762	3.41	1.5599
42	Aladja	0.99	0.0603	-2.1	-1.58
43	Itu	0.9878	0.0109	-1.99	-0.91
44	Eket	0.9919	-0.0019	-2.0	-1.47
45	Ibom GS	1.0	-0.0019	0.305	2.2952
46	Alaoji	0.9924	0.0370	-2.4	-1.0
47	Alaoji GS	1.0	0.0895	2.5	0.1307
48	Afam GS	1.0	0.0491	7.0	4.0565

Table 4: Continuation power flow (CPF) results of Nigerian 48-bus system

BUS NO	BUS NAME	VOLTAGE (pu)	PHASE ANGLE (deg)	REAL POWER (pu)	REACTIVE POWER (pu)
1	Birin Kebbi	0.9671	80.9923	-3.1179	-1.9331
2	Kainji GS	1.0000	83.4945	15.3402	3.9795
3	Kaduna	0.4505	52.4578	-3.7415	-2.8061
4	Kano	0.3613	39.714	-1.2784	-0.8107
5	Asaba	0.8244	62.0247	0.0000	0.0000
6	Makurdi	0.4527	48.3583	-3.1179	-1.8708
7	Alagbon	0.9954	-2.301	-2.1826	-1.3407
8	Lekki	0.9692	-3.1918	-3.4297	-2.432
9	Jos	0.4507	50.9567	0.0000	0.0000
10	Shiroro GS	1.0000	75.7232	15.5896	20.4486
11	Jebba	0.9533	65.5731	-8.1066	-6.0800
12	Jebba GS	1.0000	66.9195	12.5652	19.4490
13	Oshogbo	0.7666	42.3907	-3.9598	-2.9620
14	Ganmo	0.8297	56.0152	0.0000	0.0000
15	Katampe	0.9435	75.0664	-9.4473	-7.0777
16	Gwagwalada	0.9562	74.8802	0.0000	0.0000
17	Lokoja	0.9763	75.0931	0.0000	0.0000
18	Ajaokuta	0.9957	78.3379	-3.7415	-2.8061
19	Geregu GS	1.0000	78.8026	16.5562	6.8176
20	Odukpani GS	1.0000	92.7037	8.1066	3.8203

BUS NO	BUS NAME	VOLTAGE (pu)	PHASE ANGLE (deg)	REAL POWER (pu)	REACTIVE POWER (pu)
21	New heaven	0.8002	69.9862	-6.1111	-4.5834
22	Ugwuaji	0.7932	70.6709	0.0000	0.0000
23	Onitsha	0.8053	69.9203	-3.1179	-2.3384
24	Benin	0.8980	48.7994	-4.4898	-3.3674
25	Ihovbor GS	1.0000	49.0774	3.6355	16.0759
26	Adiabor	0.9774	90.508	0.0000	0.0000
27	Omosho GS	0.8155	30.2182	0.0000	0.0000
28	Ayede	0.7863	14.6255	-5.9241	-4.7081
29	Ikot Ekpene	0.9059	81.2653	-5.1446	-2.3073
30	Olorunsogo GS	0.9700	10.9736	6.1111	13.4839
31	Sakete	0.8823	-0.3599	0.0000	0.0000
32	Akangba	0.8508	-2.423	-6.3294	-4.7392
33	Ikeja West	0.8823	-0.3598	-26.4088	-19.7988
34	Okearo	0.9576	-0.1165	0.0000	0.0000
35	Aja	1.0129	-1.2141	0.0000	0.0000
36	Egbin GS	1.0330	0.0000	1.7733	54.9283
37	AES GS	1.0330	-0.0002	0.0000	0.0000
38	Okpai GS	1.0000	85.5865	14.5295	11.5664
39	Sapele GS	0.9313	50.8127	0.0000	0.0000
40	PH Main	0.9583	82.5183	-8.7302	-4.3651
41	Delta GS	1.0030	54.5985	10.6321	10.1301
42	Aladja	0.9784	53.3854	0.0000	0.0000
43	Itu	0.9309	77.3906	-6.2047	-2.8373
44	Eket	0.9451	74.808	-6.2359	-4.5834
45	Ibom GS	1.0000	74.7831	0.9600	7.7669
46	Alaoji	0.9487	82.6034	0.0000	0.0000
47	Alaoji GS	1.0000	102.2478	7.7948	1.6201
48	Afam GS	1.0000	85.915	21.8255	16.0121

Table 5: Voltage stability sensitivity factors (VSSF) of the Nigerian 48-Bus system

BUS NO	BUS NAME	VOLTAGE SENSITIVITY FACTOR
1	Birnin Kebbi	0.0228
2	Kainji GS	0.0000
3	Kaduna	0.4978
4	Kano	0.5772
5	Asaba	0.1501
6	Makurdi	0.4878
7	Alagbon	0.0272
8	Lekki	0.0454
9	Jos	0.4874
10	Shiroro GS	0.0000
11	Jebba	0.0423
12	Jebba GS	0.0000
13	Oshogbo	0.2050
14	Ganmo	0.1449
15	Katampe	0.0255
16	Gwagwalada	0.0151
17	Lokoja	0.0037
18	Ajaokuta	0.0037
19	Geregu GS	0.0000
20	Odukpani GS	0.0000
21	New heaven	0.1707
22	Ugwuaji	0.1738
23	Onitsha	0.1682
24	Benin	0.0977
25	Ihovbor GS	0.0000
26	Adiabor	0.0164

BUS NO	BUS NAME	VOLTAGE SENSITIVITY FACTOR
27	Omosho GS	0.0000
28	Ayede	0.1620
29	Ikot Ekpene	0.0760
30	Olorunsogo GS	0.0000
31	Sakete	0.0646
32	Akangba	0.1415
33	Ikeja West	0.1143
34	Okearo	0.0537
35	Aja	0.0149
36	Egbin GS	0.0000
37	AES GS	0.0000
38	Okpai GS	0.0000
39	Sapele GS	0.0000
40	PH Main	0.0291
41	Delta GS	0.0000
42	Aladja	0.0116
43	Itu	0.0570
44	Eket	0.0468
45	Ibom GS	0.0000
46	Alaoji	0.0437
47	Alaoji GS	0.0000
48	Afam GS	0.0000

Table 6: Voltage profile without and with FACTS devices

BUS NO	BUS NAME	NO FACTs	WITH TCSC	WITH SSSC
1	Birnin Kebbi	0.9899	0.9899	0.9899
2	Kainji GS	1.0	1.0	1.0
3	Kaduna	0.9482	0.9821	0.9717
4	Kano	0.9385	0.9805	0.9685
5	Asaba	0.9745	0.9771	0.976
6	Makurdi	0.9405	0.9728	0.9645
7	Alagbon	1.0225	1.0225	1.0225
8	Lekki	1.0146	1.0146	1.016
9	Jos	0.9381	0.9788	0.9668
10	Shiroro GS	1.0	1.0	1.0
11	Jebba	0.9952	0.9955	0.9954
12	Jebba GS	1.0	1.0	1.0
13	Oshogbo	0.9716	0.9755	0.9744
14	Ganmo	0.9747	0.9768	0.9762
15	Katampe	0.969	0.969	0.969
16	Gwagwalada	0.9713	0.9714	0.9713
17	Lokoja	0.98	0.9804	0.9801
18	Ajaokuta	0.9993	0.9994	0.9993
19	Geregu GS	1.0	1.0	1.0
20	Odukpani GS	1.0	1.0	1.0
21	New Heaven	0.9709	0.975	0.9732
22	Ugwuaji	0.9670	0.9725	0.9701
23	Onitsha	0.9734	0.9771	0.9755
24	Benin	0.9956	0.9961	0.9959
25	Ihovbor GS	1.0	1.0	1.0
26	Adiabor	0.9938	0.9942	0.994
27	Omosho GS	1.006	1.006	1.006
28	Ayede	0.9483	0.9648	0.9603
29	Ikotekpene	0.9819	0.9836	0.9829
30	Olorunsogo GS	0.97	0.97	0.97
31	Sakete	0.9469	0.9888	0.9803

BUS NO	BUS NAME	NO FACTs	WITH TCSC	WITH SSSC
32	Akangba	0.9923	0.9928	0.9927
33	Ikeja West	0.9966	0.9971	0.9969
34	Okearo	1.0133	1.0136	1.0135
35	Aja	1.0278	1.0278	1.0278
36	Egbin GS	1.033	1.033	1.033
37	AES GS	1.0	1.0	1.0
38	Okpai GS	1.0	1.0	1.0
39	Sapele GS	1.0	1.0	1.0
40	PH Main	0.9874	0.9874	0.9874
41	Delta GS	1.003	1.003	1.003
42	Aladja	0.99	0.99	0.99
43	Itu	0.9878	0.988	0.9879
44	Eket	0.9919	0.9919	0.9919
45	Ibom GS	1.0	1.0	1.0
46	Alaoji	0.9924	0.9926	0.9926

BUS NO	BUS NAME	NO FACTs	WITH TCSC	WITH SSSC
47	Alaoji GS	1.0	1.0	1.0
48	Afam GS	1.0	1.0	1.0
Real Power Generated		57.9435	57.8373	57.8476
Reactive power Generated		43.2527	42.7683	42.9169
Real Power Load		57.35	57.35	57.35
Reactive Power Load		39.52	39.52	39.52
Real Power Losses		0.5935	0.4873	0.4976
Reactive Power Losses		3.7327	3.2483	3.3969
% Decrease of Active Power Losses			17.884%	16.15%
% Decrease of Reactive Power Losses			12.979%	8.996%

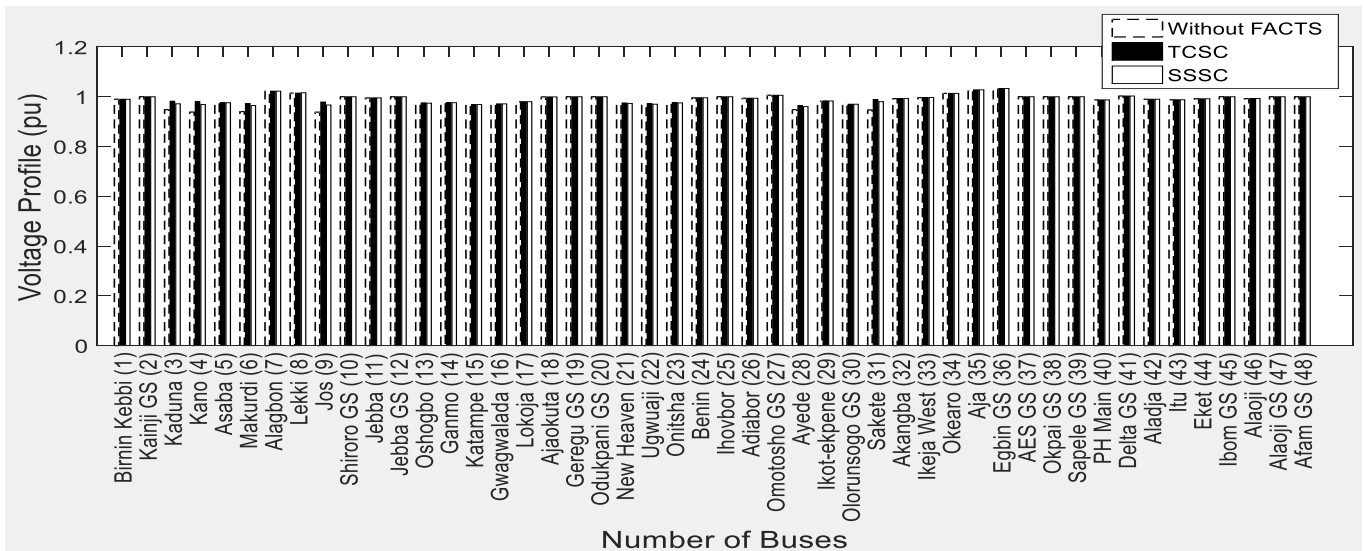


Figure 5: Voltage magnitude profile without and with TCSC and SSSC

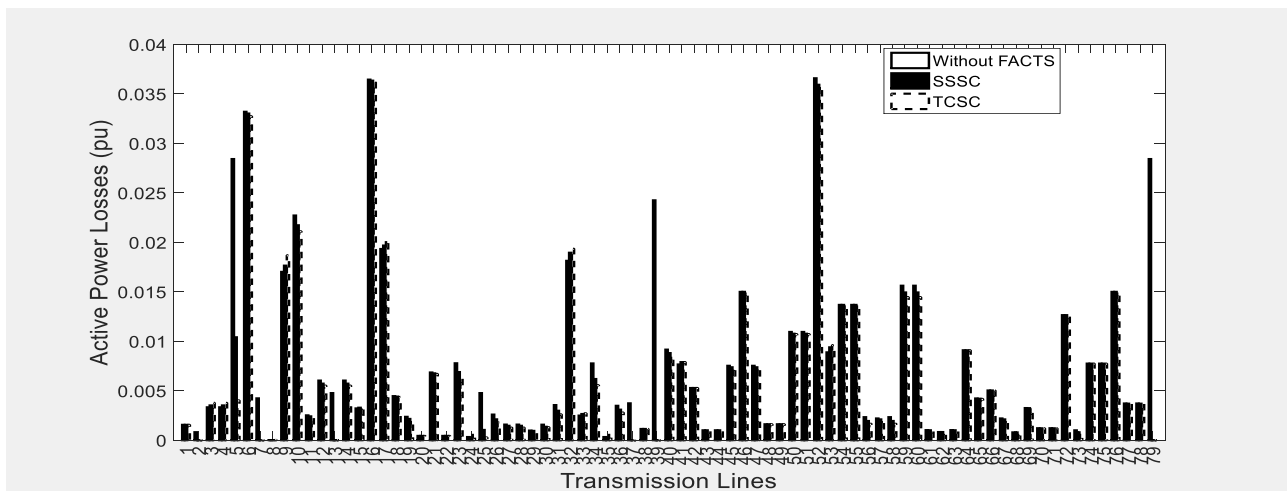


Figure 6(a): Active power losses without and with TCSC and SSSC

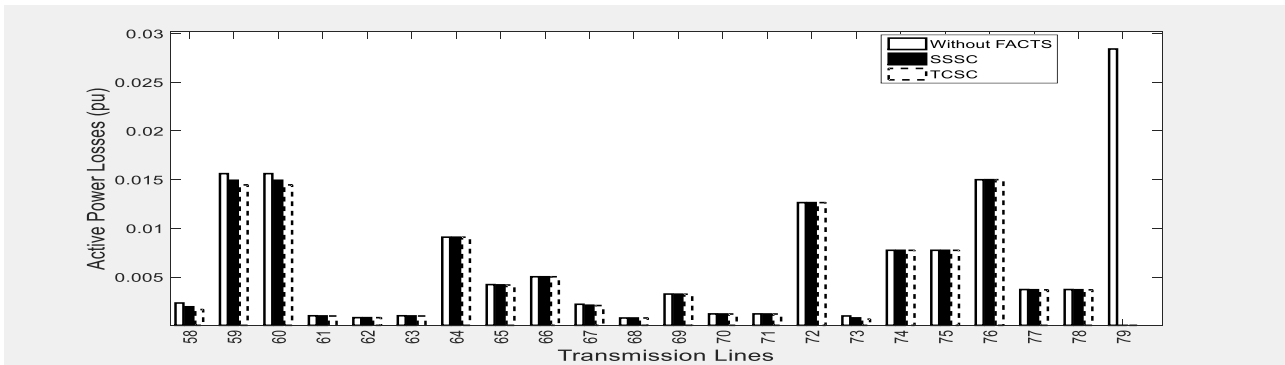


Figure 6(b): A section of Active power losses without and with TCSC and SSSC

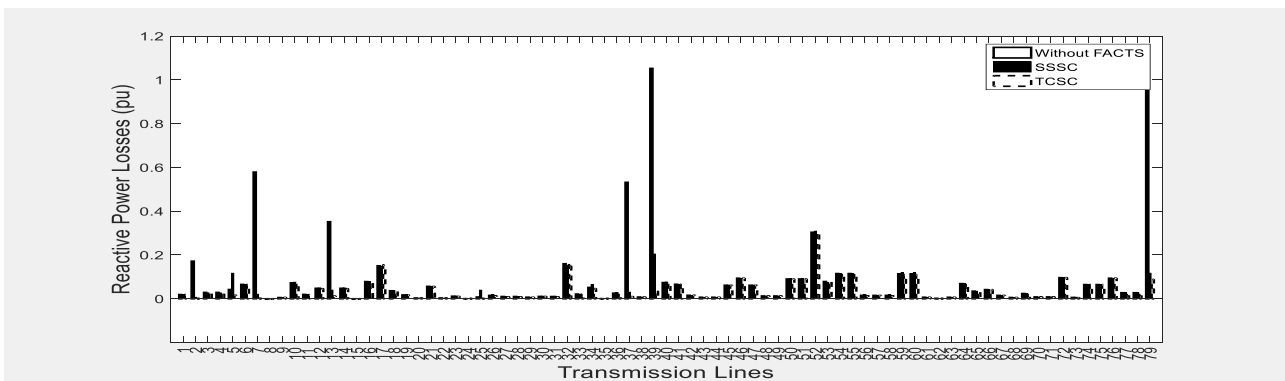


Figure 7 (a): Reactive power losses without and with TCSC and SSSC

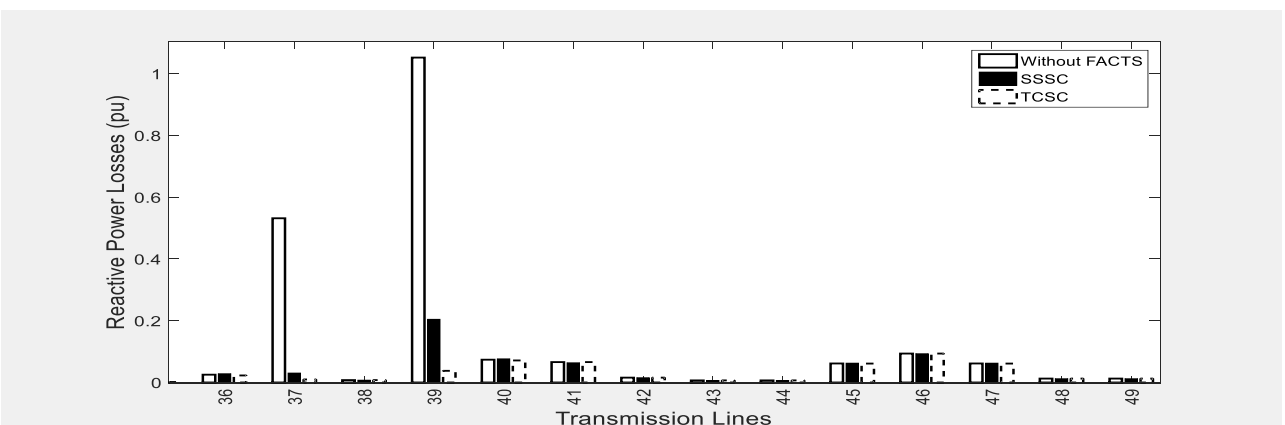


Figure 7 (b): A section of the reactive power losses without and with TCSC and SSSC

5. DISCUSSION OF RESULTS

The results of the power flow simulation of the network of Figure 3 without FACTS using Newton Raphson iteration method for power flow computations are as presented in Table 3. The iteration is completed in 0.156 second after 4 iterations with a maximum convergence error of 2.9437 e-09 p.u. and active and reactive maximum power mismatches are 2.12e -13 p.u. and 4.01e – 13 p.u. respectively. The voltage profile for the unfortified system of Figure 3 and as depicted in Table 3 shows that the following buses have voltage magnitudes

below the acceptable $\pm 5\%$ of the normal 330 kV voltage magnitude profile (1.0 p.u) [19]: 3(Kaduna), 4(Kano), 6(Makurdi), 9(Jos), 28(Ayede) and 31(Sakete). The result of the power flow also showed that the total real power generation in p.u. stands at 57.94345 p.u. and the reactive power at 43.25271 p.u. The total real power load of the system is 57.35 p.u. and the reactive power of the load is 39.52 p.u. It can also be seen that the total real power losses in pu is 0.59345 p.u. while the reactive power losses is 3.73251p.u.

From the Newton Raphson power flow of the system of Figure 3, the best position for the installation of TCSC is on line 3-4 closer to the bus with the highest VSSF which was found out to be bus 4(Kano) with 0.57724 as shown in Table 5. The result of the power flow of the network is summarized in Table 6 with the voltage magnitude profile indicated. Power flow is completed in 0.687 second after 4 iterations with a maximum convergence error of $9.6232e - 11$ p.u. and active and reactive maximum power mismatches of 1.07678 p.u. and 1.06881 p.u. respectively. The voltage levels at the buses with dips are raised up to and within $\pm 5\%$ of the acceptable value. Total real and reactive power generation for the system with TCSC is 57.94345 p.u. and 42.76825 p.u. respectively, while the losses are reduced to 0.48732 p.u. for active power and 3.24825 p.u. for reactive power.

Furthermore, the network of the Nigerian 48 bus system modeled with the installation of SSSC on line 3-4 closer to bus 4 is shown in Figure 4. The power flow of the network also summarized in Table 6 is completed in 0.156second after 4 iterations with a maximum convergence error of $1.6667 e-10$ p.u. The active and reactive maximum power mismatches are 63.19024 p.u. and 46.42357 p.u. respectively. Table 6 shows the voltage magnitude profile with SSSC indicating the improvement of the buses with voltage dips. The total active power losses reduced from 0.59345 p.u. to 0.49761 p.u. and the total reactive power losses reduced from 3.73271 p.u. to 3.39690 p.u. respectively. Graphical representation of the voltage magnitude profile of the buses is shown in Figure 5.

Figures 6 (a) and (b), 7(a) and (b) shows the comparison of the active and reactive powers of the system with and without TCSC and SSSC. Computation of the percentage decrease of the real and reactive power losses reflected the capability of the FACTS devices (TCSC and SSSC) to compensate and improve the steady state stability of the power system. From Table 6, the total active power losses dropped from 0.59345 p.u. without FACTS to 0.48732 p.u. with TCSC giving a percentage decrease of 17.884% while the reactive power dropped from 3.73271 p.u. to 3.24825 p.u.; a percentage of 12.979%. For SSSC, the total active power losses dropped from 0.59345 p.u. without FACTS to 0.49761 p.u. giving a percentage decrease of 16.15% while the reactive power dropped from 3.73271 p.u. to 3.39690 p.u.; a percentage of 8.996%.

6. CONCLUSION

The steady state stability of the Nigerian 48-bus system has been thoroughly investigated through the use of TCSC and SSSC. The parameters of the system modeled using PSAT without FACTS devices is compared with the system with TCSC and SSSC in the event of small disturbances like voltage drops as a result of long transmission lines, variation in loads etc. The FACTS devices performed creditably by enhancing stability through restoring the voltages at some buses back to an acceptable value and also mitigating against both real and reactive power losses in the system. Of the two devices, TCSC was observed to give a better compensation for effective steady state stability of the Nigerian 48-Bus system compared to SSSC.

7. REFERENCES

- [1] Kundur, P., Paserba, J., Anderson, G., Bose, A., Canizares, C., Hatziargyriou, N., Hill, D., Stankovic, A., Cutsem, T. and Vittal, V. (2004). Definition and classification of power system stability, *IEEE/CIGRE Joint Task Force on Stability Terms and Definitions IEEE Transactions on Power Systems*, 19(2): 1387-1401.
- [2] Azimoh, L. C., Folly, K. A. and Chowdhury, S. P. (2009). Mitigations of voltage instability in power systems (paper review), *IEEE Electrical Power and Energy Conference*: 1-6.
- [3] Paserba, J. J. (2003). How FACTS controllers benefit AC transmission systems, *IEEE PES Transmission and Distribution Conference and Exposition*: 991-998.
- [4] Rani, M. And Gupta, A. (2014). Steady state voltage stability enhancement of power system using FACTS devices, *6th IEEE Power India International Conference (PIICON)*: 1-6.
- [5] Sanbasiva, N. R, Amarnath, J. and Purnachandra, V. R. (2014). Effects of FACTS devices on enhancement of voltage stability in deregulated power system, *IEEE International Conference on Circuit, Power and Computing Technologies (ICCPCT)*: 642-650.
- [6] Folorunso, O., Osuji, C. C. and Ighodalo, O. S. (2014). Enhancement of power system voltage stability with the aid of reactive/capacitive power switching mechanism: (a case study of Owerri Transmission Company of Nigeria), *Journal of Advancement in Engineering and Technology*, 2(1):1-6, ISSN: 2348-2931.
- [7] Aborisade, D. O., Adebayo, I. G. and Oyesina, K. A. (2014). A comparison of the voltage enhancement and loss reduction capabilities of

STATCOM and SSSC FACTS controllers, *American Journal of Engineering Research (AJER)*, 3(1): 96-105.

- [8] Shishir, D., Ganga, A., Laxmi, S., and Ankite, S. (2014). An overview of placement of TCSC for enhancement of power system stability, *IEEE Sixth International Conference on Computational Intelligence and Communication Networks*: 1184-1187.
- [9] Bindeshwar, S., Sharma, N. K., Tiwari, A. N., Verma, K. S., and Deependra, S. (2011). Enhancement of voltage stability by coordinated control of multiple FACTS controllers in multi-machine power system environments, *IET International Conference on Sustainable Energy and Intelligent Systems*: 18-25.
- [10] Ogbuefi, U. C. and Madueme, I. C. (2015). A power flow analysis of the Nigerian 330 kV electric power system, *IOSR Journal of Electrical and Electronics Engineering (IOSR-JEEE)*, 10(1): 46-57.
- [11] Aribi, F. and Nwohu, M. N. (2014). Optimal location of STATCOM in Nigerian 330 kV network using ant colony optimization meta-heuristic, *Global Journal of Research in Engineering: F. Electrical and Electronic Engineering*, 14(3): 45-50.
- [12] Adeniji, O. A. and Mbamaluikem, P. O. (2017). Voltage stability enhancement and efficiency improvement of Nigerian transmission system using unified power flow controller, *American Journal of Engineering Research (AJER)*, 6(1): 37-43.
- [13] Adebayo, I. G., Aborisade, D. O. and Oyesina, K. A. (2013). Steady state voltage stability enhancement using static synchronous series compensator (SSSC); A case study of Nigerian 330 kV grid system, *Research Journal in Engineering and Applied Sciences*, 2(1): 54-61.
- [14] Hingorani, N. G. and Gyugyi, L. (2000). *Understanding FACTS, Concepts & Technology of Flexible AC Transmission Systems*. New York: IEEE.
- [15] Kumar, S. A., Easwarlal, C. and Kumar, S. M. (2012). Multi machine power system stability enhancement using static synchronous series compensator (SSSC), *IEEE International Conference on Computing, Electronics and Electrical Technologies (ICCEET)*: 212-217.
- [16] Faridi, M., Maeiat, H., Karimi, M., Farhadiand, P., and Mosleh, H. (2011). Power system stability enhancement using static synchronous series compensator (SSSC), *IEEE 3rd International Conference on Computer Research and Development*: 387-391.
- [17] Zhang, X., Rehtanz, C. and Pal, B. (2012). *Flexible AC Transmission System: Modeling and Control*, New York: Springer Heidelberg.
- [18] PHCN - Transmission Company of Nigeria, National Control Centre, Oshogbo, 2018.
- [19] Ayodele, T. R., Ogunjuyigbe, A. S. O. and Oladele, O. O. (2016). Improving the transient stability of Nigerian 330 kV transmission network using static var compensation part 1: the base study, *Nigerian Journal of Technology (NIJOTECH)*, 35(1): 155-166.